A Leucine Zipper Motif in the Ectodomain of Sendai Virus Fusion Protein Assembles in Solution and in Membranes and Specifically Binds Biologically-Active Peptides and the Virus†

Jimut Kanti Ghosh,‡ Michael Ovadia,§ and Yechiel Shai*,‡

Department of Membrane Research and Biophysics, The Weizmann Institute of Science, Rehovot, 76100 Israel and Department of Zoology, George S. Wise Faculty of Life Sciences, Tel Aviv University, Ramat Aviv, 69978 Israel

Received May 16, 1997; Revised Manuscript Received October 13, 1997⊗

ABSTRACT: We have detected a leucine zipper-like motif in the ectodomain of the Sendai virus fusion protein (aa 269−307) which is extremely conserved in the family of Sendai viruses. To find a possible role for this motif, we synthesized SV-269, a 39 amino acid peptide corresponding to this domain, and a mutant peptide, MuSV-269, with an amino acid pair interchanged their positions. The peptides were labeled with fluorescent probes at their N-terminal amino acid and functionally and structurally characterized. The data show that SV-269, but not MuSV-269, specifically binds Sendai virus. Expectedly, SV-269 is more active than the mutant MuSV-269 in inhibiting Sendai virus-mediated hemolysis. Fluorescence studies reveal that SV-269 assembles in aqueous solution, binds to zwitterionic PC and negatively-charged PS/PC vesicles, and assembles therein. Although MuSV-269 similarly binds to both types of vesicles, it only slightly assembles in solution and not at all in membranes. Moreover, SV-269, but not MuSV-269, coassembles with the biologically-active heptad repeats SV-150 and SV-473 (Rapaport et al., 1995) in solution as revealed by fluorescence and circular dichroism (CD) spectroscopy, and with SV-150 within negatively-charged PS/PC and zwitterionic PC vesicles. Despite these differences, both SV-269 and MuSV-269 adopt similar secondary structures in 40% TFE and 1% SDS as revealed by CD spectroscopy, and disrupt the packing of the lipid bilayers to the same extent, as shown by the dissipation of diffusion potential. The role of this leucine zipper motif is discussed in terms of the assembly of the Sendai virus fusion protein in solution and within membranes. Since most of the heptadic leucines are also conserved in the corresponding domains of other paramyxoviruses such as rinderpest, measles, SV5, and parainfluenza, it may indicate a similar role of this domain in these viruses as well.

The entry of enveloped viruses into host cells is accomplished by membrane fusion which involves the fusion of the viral envelope and target plasma membrane (*1*−3). Membrane fusion is mediated by several glycoproteins present in the viral envelope. Sendai virus, which belongs to the paramyxovirus family, has two envelope glycoproteins (*4*); the hemagglutinin/neuraminidase, HN, glycoprotein which possesses the receptor-binding activity of the virus to the sialic acid containing cell surface (*5, 6*), and the fusion protein, F, which is assumed to be directly involved in the membrane fusion process. The ability of the F protein to mediate fusion is associated with the proteolytic cleavage of an inactive precursor, F0, by a host enzyme, to yield two disulfide-linked polypeptides, F1 and F2 (*7*−*9*). During this cleavage, a new N-terminus on the F1 is liberated which is very hydrophobic and highly conserved among different paramyxoviruses. Although this new N-terminus, known as "fusion peptide", is believed to make the primary contact with the target membrane, it is unlikely that it is solely responsible for the fusion process. Indeed, recent studies demonstrate the involvement of heptad repeat regions, some of which have a leucine zipper-like sequence, in virus−cell fusion.

Leucine zippers are a special class of heptad repeats which contain leucine or isoleucine at every seventh amino acid residue (*10, 11*). The leucine zipper motif was first described in several DNA-binding proteins including transcriptional regulators (e.g., yeast GCN4 and mammalian C/EBP) and nuclear transforming proteins such as Jun, Fos, and Myc (*12*). The leucine zipper motifs in these proteins are believed to participate in their dimerization to create a DNA-binding site. A synthetic peptide model has demonstrated that a leucine zipper sequence can associate into noncovalent, parallel helical dimers (*11*). The predicted coiled-coil structure of a leucine zipper motif has been proven by X-ray studies (*13*). Since oligomerization is an essential feature of the fusogenic viral glycoproteins, it has been postulated that the leucine zipper motif could contribute to the oligomeric structures of these viral proteins. Recently, Bernstein et al. have demonstrated the oligomerization of a classical monomeric protein following fusion with a heptad repeat sequence present in the HIV transmembrane glycoprotein gp41 (*14*). On the basis of very similar results, it has been proposed that the fusogenic structure of gp41 involves tetramerization of the leucine zipper domain, situated near the fusion peptide

†This research was supported in part by the Henri and Francoise Glasberg Foundation. J.K.G. acknowledges the receipt of a Sir Charles Clore postdoctoral fellowship from the Feinberg Graduate School, The Weizmann Institute of Science.

* To whom correspondence should be addressed at the Department of Membrane Research and Biophysics, The Weizmann Institute of Science, Rehovot, 76100 Israel. Telephone: 972-8-9342711. Fax: 972-8-9344112. Email: bmshai@weizmann.weizmann.ac.il.

‡ The Weizmann Institute of Science.

§ Tel Aviv University.

⊗ Abstract published in *Advance ACS Abstracts,* December 1, 1997.

S0006-2960(97)01152-5 CCC: $14.00

(*15*). Previously, it has been shown that mutations in this leucine zipper motif do not abolish the ability of HIV envelope protein to oligomerize but do affect the fusion activity of the virus, suggesting that this conserved leucine zipper has an important role in the virus life cycle (*16*). Paramyxoviruses have more than one leucine zipper motif. Bukland et al. reported that mutations in the leucine zipper positioned near the fusion peptide of the measles virus prevent fusion without affecting the cellular transport and oligomerization of the F protein (*17*). Similarly, mutations that replace the conserved leucines in the leucine zipper motif near the transmembrane domain of the Newcastle disease virus, a paramyxovirus, drastically reduce the fusogenic ability of the protein without altering its oligomeric state (*18*). Furthermore, synthetic heptad repeat regions corresponding to different domains of the HIV transmembrane gp41 (*19, 20*), Sendai virus fusion protein (*21*), and three other paramyxoviruses (*22*) inhibit virus mediated cell−cell fusion. The antiviral activity of these peptides is believed to be due to their ability to accurately model and interact with functional domains of the proteins. In addition to its role in oligomerization, it has been proposed that a loop region of the influenza hemagglutinin containing a leucine zipper motif is associated with the fusogenic conformation of the whole protein (*23*). The observation that the synthetic peptides corresponding to leucine zipper motifs in influenza hemagglutinin (*24*) and Sendai virus (*21*) can interact with the lipid membrane suggests that these domains are involved in membrane apposition.

We have identified a leucine zipper-like motif, designated SV-269, in the ectodomain of the Sendai virus fusion protein. This region is in addition to two other leucine zipper motifs in paramyxoviruses, one positioned near the fusion peptide and the another near the transmembrane anchor domain. SV-269 is extremely conserved in the family of Sendai viruses and is positioned in between the two heptad repeats in the Sendai virus fusion protein. Furthermore, most of the heptadic leucines/isoleucines are conserved in other members of paramyxoviruses, suggesting a similar role in the corresponding fusion proteins. We synthesized the wild-type SV-269, as well as a mutant peptide, MuSV-269, with only two amino acids (one heptadic leucine and a glutamic acid), interchanged in their positions. The peptides were further labeled with fluorescent probes to study their ability to bind virions and to inhibit Sendai virus mediated hemolysis, their aggregation states in aqueous solution, their ability to bind phospholipid vesicles and to assemble therein, and their ability to coassemble with the biologically-active heptad repeats SV-150 and SV-473. The results are discussed in terms of the role of the SV-269 region in the assembly of the Sendai virus fusion protein.

MATERIALS AND METHODS

Materials. BOC-ser-PAM[1] resin was purchased from Applied Biosystems (Foster City, CA), and BOC amino acids were obtained from Bachem (Switzerland). Other reagents for peptide synthesis included trifluoroacetic acid (TFA) (Sigma), *N,N*-diisopropylethylamine (DIEA) (Aldrich, distilled over ninhydrin), dicyclohexylcarbodiimide (DCC) (Fluka), and 1-hydroxybenzotriazole (HOBT) (Pierce). Egg phosphatidylcholine (PC) and phosphatidylserine (PS) from bovine spinal cord (sodium salt, grade I) were purchased from Lipid Products (South Nutfield, U.K). 3,3′-Diethylthiodicarbocyanine iodide (diS-C_2-5), NBD-F (4-fluoro-7-nitro-2,1,3-benzoxadiazole), and tetramethylrhodamine succinimidyl ester were obtained from Molecular Probes (Eugene, OR). All other reagents were of analytical grade. Buffers were prepared in double glass-distilled water.

Peptide Synthesis, Fluorescent Labeling, and Purification. The peptides were synthesized by a solid-phase method on the corresponding resins (0.15 mequiv), as previously described (*25, 26*). Double coupling was carried out with freshly prepared hydroxybenzotriazole (HOBT)-active esters of BOC amino acids. Labeling of the N-terminus of a peptide was achieved as reported previously (*27*). Briefly, 15 mg of a resin-bound peptide in its fully protected form was treated with TFA (50% v/v in methylene chloride) to remove the BOC protecting group from the N-terminal amino groups of the linked peptides. The resin-bound peptides were then treated with either (i) tetramethylrhodamine succinimidyl ester (3−4 equiv) in dry dimethylformamide containing 5% v/v diisopropylethylamine or (ii) NBD-fluoride (2−3 equiv) in dry dimethylformamide, which led to the formation of resin-bound N^1-Rho or N^1-NBD peptides, respectively. After 48 h, the resins were washed thoroughly with DMF and then with methylene chloride to remove unreacted fluorescent probes. The peptides were then cleaved from the resins by HF and finally precipitated with ether. All the peptides were purified using RP-HPLC on an analytical C_4 reversed-phase Vydac column (300 Å pore size). The column was eluted in 40 min, using a linear gradient of 25−80% acetonitrile in water [both containing 0.05% TFA (v/v)], at a flow rate of 0.6 mL/min. The purified peptides were shown to be homogeneous (∼99%) by analytical HPLC. The peptides were subjected to amino acid analysis.

Virus and Erythrocytes. Sendai virus (Z strain) was grown in the allantoic sac of 10−11 day old embryonated chicken eggs, harvested 48 h after injection, and purified according to Peretz et al. (*28*). The virus was resuspended in buffer composed of 160 mM NaCl, 20 mM tricine, pH 7.4, and stored at −70 °C. The activity of virions was expressed in hemagglutinating units (HAU) as described earlier (*28*).

Human blood was obtained from a blood bank and used fresh. Prior to use, erythrocytes were washed twice with phosphate-buffered saline (PBS), pH 7.3, and diluted to the desired concentration (% v/v) with the same buffer.

Assay of Sendai Virus Induced Human RBC Hemolysis and Its Inhibition by SV-269 and MuSV-269. Virions and erythrocytes alone or virions and erythrocytes and peptides at various amounts were mixed together. The final incubation was always at 37 °C for 40 min, followed by centrifugation at 5700*g* for 8 min to remove intact cells. In all assays, duplicate samples were used and two aliquots taken from the supernatant of each sample were placed in two wells of a 96-well plate. The amount of hemoglobin released was monitored by measuring the absorbance of the wells by using an ELIZA plate reader at 540 nm.

[1] Abbreviations: BOC, butyloxycarbonyl; CD, circular dichroism; diS-C_2-5, 3,3′-diethylthiodicarbocyanine iodide; DMSO, dimethyl sulfoxide; HF, hydrogen fluoride; NBD-F, 4-fluoro-7-nitro-2,1,3-benzoxadiazole; Pam, phenylacetamidomethyl; PC, egg phosphatidylcholine; PS, phosphatidylserine; PBS, phosphate-buffered saline (pH 7.3); RP-HPLC, reverse-phase high-performance liquid chromatography; Rho, tetramethylrhodamine; RET, resonance energy transfer; SUVs, small unilamellar vesicles; TFA, trifluoroacetic acid; TFE, trifluoroethanol.

Preparation of Small Unilamellar Vesicles (SUVs). SUVs were prepared by sonication of PC or PS/PC (1:1 w/w), as described previously (*29*). In brief, dry lipids were dissolved in $CHCl_3$/MeOH (2:1 v/v). The solvents were evaporated under a stream of nitrogen, and the thin film of lipids formed was resuspended in PBS buffer (at a concentration of 7.2 mg/mL) by vortex mixing. The resulting lipid dispersions were sonicated (10−30 min) in a bath-type sonicator (G1125SP1 Sonicator; Laboratory Supplies Co. Inc., New York) until the turbidity had cleared. The lipid concentrations of the resulting preparations were determined by phosphorus analysis (*30*). Vesicles were visualized using a JEOL JEM 100B electron microscope (Japan Electron Optics Laboratory Co., Tokyo, Japan) by depositing a drop of vesicles on a carbon-coated grid and negatively staining them with uranyl acetate. Examination of the grids demonstrated that the vesicles were unilamellar, with an average diameter of 20−50 nm (*31*).

CD Spectroscopy. The CD spectra of the peptides were measured in PBS buffer, 40% TFE in water, and 1% SDS in water, using a Jasco J-500A spectropolarimeter that had been calibrated with (±)-10-camphorsulfonic acid. The samples were scanned at 23 °C in a capped quartz optical cell with a 0.2 cm path length. Spectra were obtained at wavelengths of 250−190 nm. An average of 8−12 scans were taken for each sample at a scan rate of 10 nm/min, with a sampling interval of 0.2 nm and a peptide concentration of 8−12 μM. The fractional helicities (*32*, *33*) were calculated as follows:

$$f_h = \frac{[\theta]_{222} - [\theta]^0_{222}}{[\theta]^{100}_{222} - [\theta]^0_{222}}$$

where $[\theta]_{222}$ was the experimentally observed mean residue ellipticity at 222 nm, and the values for $[\theta]^0_{222}$ and $[\theta]^{100}_{222}$, which correspond to 0% and 100% α-helix content at 222 nm, were estimated as −2000 and −32 000 deg·cm^2/dmol, respectively (*33*).

Binding Experiments. Binding experiments were conducted as previously described (*34*). Briefly, SUVs were added gradually to 0.1−0.2 μM of NBD-labeled peptides at room temperature. Fluorescence intensities were measured as a function of the lipid:peptide molar ratios on a Perkin-Elmer LS-50B spectrofluorometer, with the excitation set at 467 nm, using a 10 nm slit, and the emission set at 530 nm, using a 5 nm slit, in three separate experiments. The extent of the lipids' contribution to any given signal was determined using readings obtained when unlabeled peptides were titrated with lipid vesicles, and were subtracted as backgrounds from the recorded fluorescence intensities. The binding isotherms were analyzed as partition equilibria (*35*, *36*, *34*), using the formula:

$$X_b^* = K_p^* C_f$$

where X_b^* is defined as the molar ratio of bound peptide per 60% of the total lipid, assuming that the peptides were initially partitioned only over the outer leaflet of the SUV, as has been previously suggested (*36*), K_p^* corresponds to the partition coefficient, and C_f represents the equilibrium concentration of the free peptide in the solution. X_b was calculated by extrapolating F_∞ (the fluorescence signal obtained when all the peptide is bound to lipid) from a double-reciprocal plot of F (total peptide fluorescence) versus C_L (total concentration of lipids) (*35*). Knowing the fluorescence intensities of unbound peptide, F_0, as well as bound peptide, F, the fraction of membrane-bound peptide, f_b, could be calculated using the formula:

$$f_b = (F - F_0)/(F_\infty - F_0)$$

After calculating the value of f_b, it is then possible to calculate C_f, as well as the extent of peptide binding, X_b^*. The curves that result from plotting X_b^* versus free peptide, C_f, are referred to as the conventional binding isotherms.

Enzymatic Cleavage Experiments. To determine the susceptibility of the peptides to proteolytic degradation in their membrane-bound state, enzymatic cleavage experiments were done as described previously (*21*). Briefly, lipid vesicles composed of either PC or PS/PC were added to a NBD-labeled peptide in PBS buffer followed by the addition of 5 μL of proteinase K (0.5 mg/mL). The time profiles of the emission were recorded at 530 nm (slit 10 nm) with excitation set at 467 nm (slit 10 nm) using a Perkin-Elmer LS-50B spectrofluorometer. In these experiments, the peptide:lipid molar ratio was kept at such a level so that the major portion of the NBD-labeled peptide was bound to membranes. In a control experiment, the enzyme was added to NBD-labeled peptide prior to the addition of lipid vesicles.

Resonance Energy Transfer Measurements. Fluorescence spectra were obtained at room temperature on a Perkin-Elmer LS-50B spectrofluorometer, with the excitation monochromator set at 467 nm with a 5−8 nm slit width. Measurements were performed in a 0.5 cm path-length glass cuvette in a final reaction volume of 0.4 mL. In a typical experiment, the desired amount of a donor peptide was added to a dispersion of SUVs in PBS buffer, followed by the addition of an acceptor peptide, either in a single or in several sequential doses. Fluorescence spectra were recorded before and after the addition of the acceptor. Changes in the fluorescence intensity of the donor due to processes other than energy transfer to the acceptor were determined by using unlabeled peptide instead of the acceptor.

The efficiency of energy transfer (E) was determined by the decrease in the quantum yield of the donor as a result of the addition of the acceptor. E was determined experimentally from the ratio of the fluorescence intensities of the donor in the presence (I_{da}) and in the absence (I_d) of the acceptor at the emission wavelength of the donor, after correcting for membrane light scattering and the contribution of the emission of the acceptor. The percentage of E is given by the equation:

$$E = (1 - I_{da}/I_d) \times 100$$

The correction for light scattering was made by subtracting the signal obtained when unlabeled peptides, at concentrations equal to the sum of the donor and the acceptor, were added to vesicles. Correction for the contribution of the acceptor emission was made by subtracting the signal produced by the acceptor-labeled peptide alone.

Membrane Permeability Assay. Membrane destabilization, which results in the collapse of a diffusion potential, was detected fluorometrically, as previously described (*37*, *38*). In brief, a liposome suspension, prepared in "K^+ buffer" (50 mM K_2SO_4/25 mM HEPES−sulfate, pH 6.8), was added to

Table 1: Sequence Alignment of Amino Acids 269−307 of Sendai Virus[a]

	1	10	20	30
Sendai virus	IKGTVIDVD**L**ERYMVT**L**SVKIPI**L**SEVPGV**L**IHKASS**I**S			
Rinderpest virus	IKAKITYVD**I**ESYFIV**L**SIAYPS**L**SEIKGV**I**VHRLEGVS			
Measles virus	IKARITYVD**I**ESYFIV**L**SIAYPT**L**SEIKGV**I**VHRLEGVS			
Parainfluenza virus	VKGTVIDVD**L**EKYMVT**L**LVKIPI**L**SEIPGV**L**IYRASS**I**S			
SV5	LTGQIVGLD**L**TYMQMV**I**KIELPT**L**TVQPATQIIDLAT**I**S			

[a] Underlined amino acids are conserved in Sendai virus and other viruses.

an isotonic K^+-free buffer (50 mM Na_2SO_4/25 mM HEPES−sulfate, pH 6.8), and the dye diS-C_2-5 was then added. Subsequent addition of valinomycin created a negative diffusion potential inside the vesicles by a selective efflux of K^+ ions, which resulted in a quenching of the dye's fluorescence. Peptide-induced membrane permeability for all the ions in the solution caused a dissipation of the diffusion potential, as monitored by an increase in fluorescence. Fluorescence was monitored using excitation and emission wavelengths at 620 and 670 nm, respectively. The percentage of fluorescence recovery, F_t, was defined by

$$F_t = [(I_t - I_o)/(I_f - I_o)] \times 100\%$$

where I_t = the fluorescence observed after addition of a peptide at time t, I_o = the fluorescence after addition of valinomycin, and I_f = the total fluorescence prior to the addition of valinomycin.

RESULTS

We detected a highly conserved leucine zipper motif in the ectodomain of the Sendai virus fusion protein which also has a considerable amino acid homology with other paramyxoviruses (Table 1). Particularly, SV-269 has 80% sequence homology with the equivalent region in parainfluenza virus, although the lengths of the extracellular domains of their fusion proteins are significantly different. It appears from the sequence alignment (Table 1) that the heptad leucines or isoleucines of this domain are conserved in the corresponding domains of other paramyxoviruses. To examine a possible role of this leucine zipper-like region, we have synthesized, fluorescently labeled with NBD (to serve in the binding studies and as an energy donor) and rhodamine (to serve as an energy acceptor), and structurally and functionally characterized SV-269, a 39 residue peptide, corresponding to this domain, and MuSV-269, a mutant peptide with 1 pair of amino acids interchanged in their positions. Table 2 shows the sequences of the peptides, and Figure 1A,B shows the location and the helical wheel structures of SV-269 and MuSV-269, respectively.

SV-269, but Not MuSV-269, Assembles in Solution in a Dose-Dependent Manner. All the viral fusion proteins exist as oligomers in the fusogenic or prefusogenic states (*39*). The possibility that the 269−307 aa domain may be involved in the assembly of the fusion protein in the native state was examined by measuring the ability of the peptides to self-associate in solution. Since the fluorescence of Rho or NBD is quenched when several molecules are in close proximity, a difference in the fluorescence intensity between equal concentrations of fluorescently labeled wild-type and mutant peptides can indicate a difference in their aggregational states.

Table 2: Amino Acid Sequences of the Peptides Used and Their Fluorescently Labeled Analogues[c]

No.	Designation	Sequence
1	SV-269	X-NH-IKGTVIDVD**L**ERYMVT**L**SVKIPI**L**SEVPGV**L**IHKASSIS-COOH
2	MuSV-269	X-NH-IKGTVIDVD**LL**RYMVT**E**SVKIPI**L**SEVPGV**L**IHKASSIS-COOH
3	SV-163[a]	X-NH-KSVELLQNAVGEQILALKTLQDFV-COOH
4	SV-150[b]	X-NH-DIALIKESMTKTHKSVELLQNAVGEQILALKTLQDFV-COOH
5	SV-473[a]	X-NH-FLQDSKAELEKAARKILSEVGRWY-COOH

[a] Taken from (21). [b] Taken from Ben-Efraim et al. (unpublished results). [c] Underlined amino acids in sequence 2 exchanged their positions. X = H, NBD, or rhodamine.

The dose response fluorescence of both Rho-SV-269 and Rho-MuSV-269 peptides was recorded at 575 nm (emission maxima of Rho) and was plotted versus the concentrations of the peptides (figure not shown). Identical results were obtained with both Rho and NBD. We observed that above 0.05 μM, the plot of wild-type Rho-SV-269 deviates sharply from linearity while that of Rho-MuSV-269 is linear up to the maximal concentration tested. The nonlinearity of the curve of wild-type SV-269 is presumably due to its tendency to aggregate in solution. The linear nature of curve of Rho-MuSV-269 suggests that the mutant exists mostly in a monomeric state in aqueous solution.

The difference in the aggregation state between wild-type SV-269 and mutant MuSV-269 is also evident from the fluorescence level of rhodamine-labeled peptides following complete enzymatic digestion. As expected, when approximately the same concentrations (0.45 μM) of Rho-SV-269 and Rho-MuSV-269 were dissolved in methanol, a solvent which does not promote aggregation of the peptides, the peptides exhibited the same fluorescence (data not shown). However, when the peptides were added to PBS, the fluorescence of Rho-MuSV-269 was two-fold higher than that of Rho-SV-269, which indicates that Rho-SV-269 is in a higher aggregational state than Rho-MuSV-269. However, the addition of proteinase K to solutions of Rho-SV-269 and Rho-MuSV-269 resulted in similar levels of fluorescence for both peptides, which was only ∼20% above the fluorescence of Rho-MuSV-269 in buffer (data not shown). This result confirms that the lower fluorescence level of Rho-SV-269 is due to its higher aggregational state in aqueous solution as compared to the mutant peptide.

The reversible nature of the self-association of SV-269 in solution was demonstrated by the increase in the fluorescence of Rho-SV-269, upon the addition of unlabeled SV-269 (Figure 2A). The specificity of the association is further confirmed by the finding that the addition of the same amount of unlabeled MuSV-269 peptide did not cause any increase in the fluorescence of Rho-SV-269 (Figure 2A).

Coassembly of SV-269 with Biologically-Active Heptad-Repeat Regions. It was of interest to know whether the SV-269 leucine zipper region could also coassemble with two biologically-active heptad-repeat domains of Sendai virus fusion protein, namely, SV-473 (*21*) and SV-150 (Ben-Efraim et al., unpublished results). SV-150, composed of aa 150−186, is an elongated version of the biologically-inactive SV-163 peptide (*21*), and it inhibits virus-mediated erythrocyte hemolysis at doses ∼30% that of SV-473. Recent studies using CD spectroscopy demonstrated that SV-150 and SV-473 can coassemble in solution (Ben-Efraim et

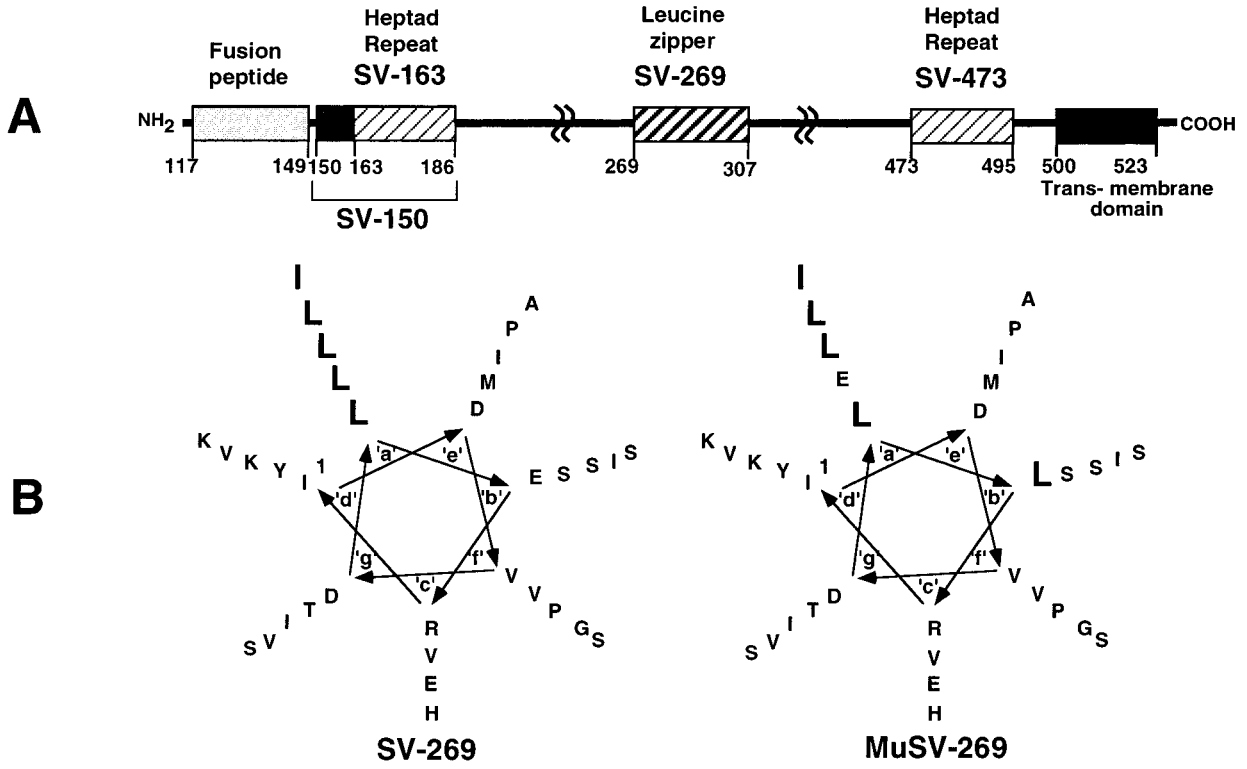

FIGURE 1: (A) Schematic representation of the F_1 fusion protein of Sendai virus. (B) Helical-wheel projections of SV-269 and MuSV-269 beginning with isoleucine (at position 274) at position 'd'. Heptad leucines/isoleucines are marked by boldface letters.

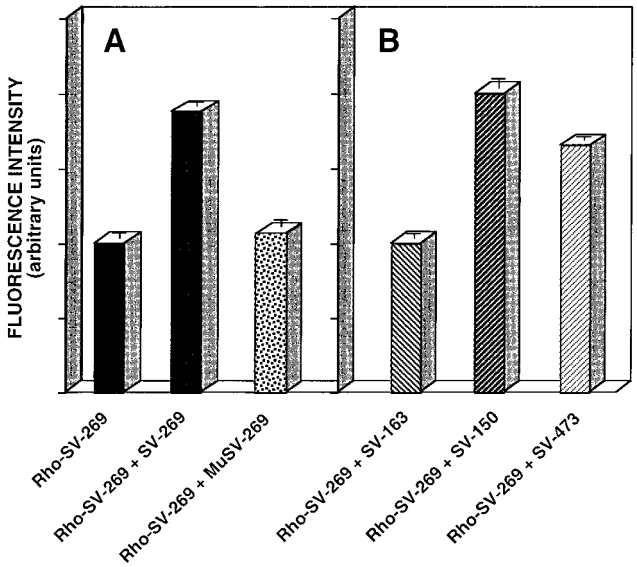

FIGURE 2: Determination of the nature of self-assembly (panel A) and coassembly of SV-269 with heptad repeats (panel B) in an aqueous environment by monitoring the dequenching of rhodamine fluorescence of Rho-SV-269, followed by the addition of different unlabeled peptides. In all the experiments, the concentration of Rho-SV-269 was fixed at 0.025 μM, and the concentrations of unlabeled SV-269, MuSV-269, SV-473, and SV-150 were 0.16 μM each while the concentration of SV-163 was 0.10 μM.

al., unpublished results) similarly to what has been found with homologous heptad repeat regions in gp41 (*40*). When unlabeled heptad repeats were added to Rho-SV-269, an increase in the fluorescence of Rho-SV-269 was observed only with the biologically-active SV-150 and SV-473, but not with the biologically-inactive SV-163 (Figure 2B). Moreover, no increase in fluorescence was observed when Rho-MuSV-269 was substituted for Rho-SV-269 (data not shown).

To get further evidence for the ability of SV-269 to coassemble with SV-150 and SV-473, circular dichroism experiments were performed. CD spectra of SV-269 and MuSV-269 were recorded separately and in the presence of the two heptad repeats in aqueous environment. In order to assess the interaction of SV-269 and MuSV-269 with the heptad repeats, the algebric sum of the individual CD spectra of each pair was compared to the experimental spectra recorded after mixing them together in aqueous solution. Figure 3 shows an increase in the intensity of experimental CD spectra of SV-269 mixed with SV-473 (Figure 3A) and SV-150 (Figure 3C), as compared to their algebric sum. However, in the case of MuSV-269 (Figure 3B,D), the difference between the algebric sum of the individual spectra of each pair and the experimental spectra when they were mixed together was not significant. These results further support the notion that SV-269 interacts with SV-473 and SV-150 in solution, whereas the mutant peptide MuSV-269 does not. Presumably their interaction is associated with an increase in the helix content of the resultant complex.

Both SV-269 and MuSV-269 Bind to Phospholipid Membranes. The sensitivity of the NBD moiety to the dielectric constant of its surroundings facilitates the determination of the environment of NBD-labeled polypeptide in its membrane-bound state. This probe has previously been used in polarity and binding experiments (*41*, *42*, *34*, *43*). The fluorescence emission spectra of NBD-labeled wild-type and MuSV-269 peptides were measured in aqueous solution and in the presence of PC or PS/PC vesicles. Both the wild-type and mutant NBD-labeled peptides exhibited fluorescence emission maxima around 540 nm in buffer, which is in agreement with the previously reported emission maxima for NBD derivatives in hydrophilic environments (*44*, *34*, *43*). However, the addition of PC or PS/PC vesicles in PBS, pH 7.3, resulted in a blue shift of the fluorescence emission maxima

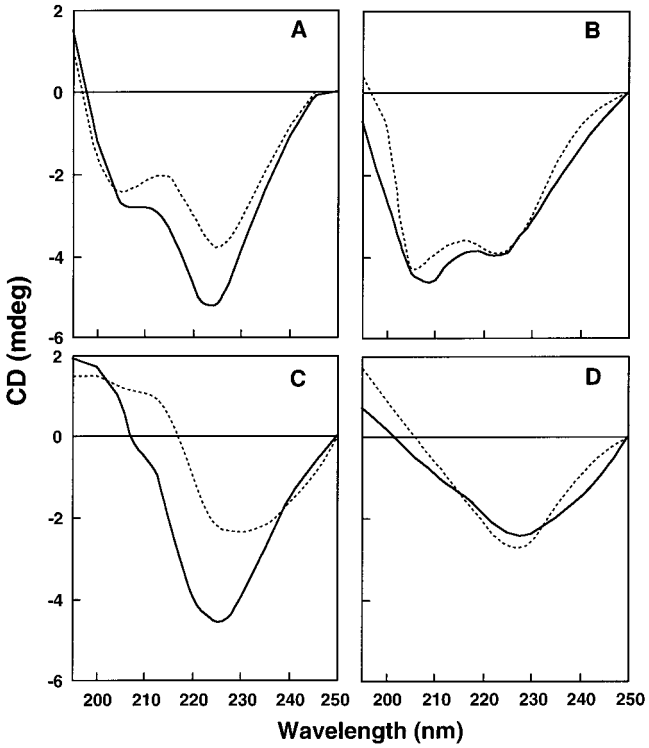

FIGURE 3: Detection of coassembly of SV-269 and MuSV-269 with the heptad repeats SV-150 and SV-473 in aqueous environment by circular dichroism experiments. CD results were expressed in millidegrees vs wavelength (in nanometers). Concentrations of SV-269 and MuSV-269 were fixed at 8.5 μM whereas SV-473 and SV-150 concentrations were 10.3 and 8.8 μM, respectively. CD experiments were performed for each peptide separately or in combinations of the two peptides, keeping the concentration of the peptides unchanged. The algebric sum was calculated from the individual spectra of the peptides. Designations: solid lines, mixtures of peptides; dotted lines, algebric sums. Panel A: SV-269 and SV-473. Panel B: MuSV-269 and SV-473. Panel C: SV-269 and SV-150. Panel D: MuSV-269 and SV-150.

of both NBD-labeled peptides, with significant enhancement of fluorescence (figure not shown). These blue shifts and increased fluorescence are due to the relocation of the NBD moiety to a more hydrophobic environment. Both the wild-type and mutant NBD-labeled peptides exhibited identical blue shifts around 527 nm in PS/PC and in PC vesicles, which suggests that the N-terminals of both peptides are located in similar environments, close to the surface of the membrane. These data show that SV-269 interacts with both zwitterionic PC and negatively-charged PS/PC vesicles and that the mutation in the leucine zipper motif does not affect binding to lipid bilayers. To avoid the spectral contribution of the free peptide in these experiments, a high lipid:peptide molar ratio was consistently maintained.

Determination of Binding Isotherms and Partition Coefficients. The affinity of SV-269 and MuSV-269 for phospholipid membranes was determined by binding experiments using their corresponding NBD-labeled analogues. Conventional binding curves were generated by plotting the increases in the fluorescence intensities of the NBD-labeled peptides following the addition of either PC or PS/PC vesicles as a function of lipid:peptide molar ratios (Figure 4A). Binding isotherms were analyzed as partition equilibria as described under Materials and Methods. The curves resulting from plotting X_b* versus free peptide, C_f, are referred to as the conventional binding isotherms and are presented in Figure 4B. The surface partition coefficient of

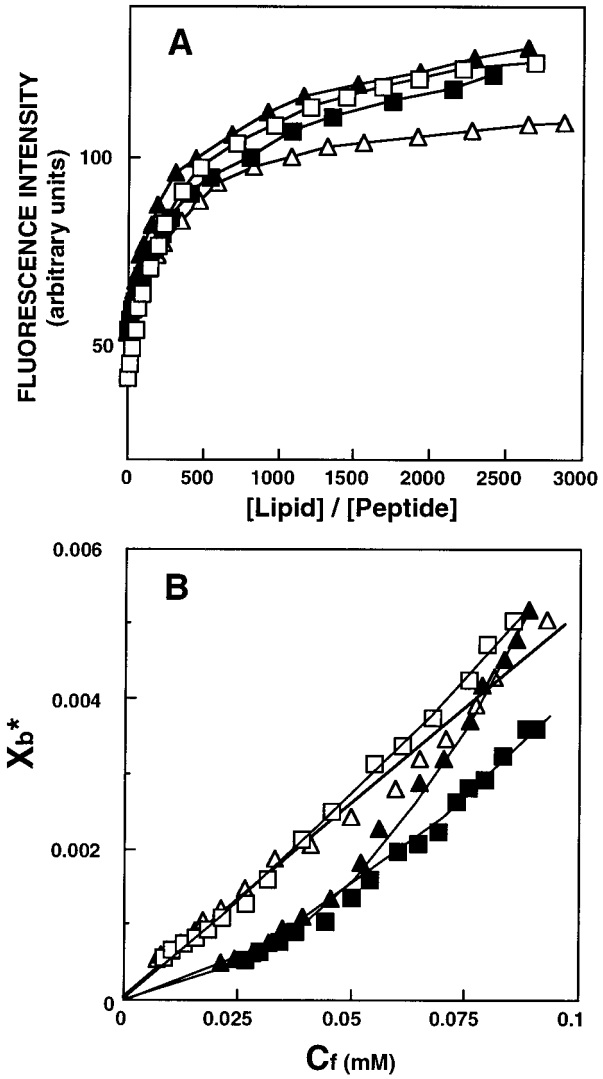

FIGURE 4: Increase in the fluorescence of NBD-SV-269 (0.10 μM) and NBD-MuSV-269 (0.09 μM) upon titration with PS/PC and PC vesicles (panel A), and the resulting binding isotherms (panel B). Titration was performed at room temperature in buffer composed of 150 mM NaCl, 10 mM sodium phosphate, pH 7.3. The excitation wavelength was set at 470 nm, and emission was recorded at 530 nm. The binding isotherms were derived from panel A by plotting X_b* (molar ratio of bound peptide per 60% lipid) versus C_f (equilibrium concentration of free peptide in the solution). Symbols: open triangles, SV-269 in PC; open squares, MuSV-269 in PC; closed triangles, SV-269 in PS/PC; closed squares, MuSV-269 in PS/PC.

each peptide, K_p*, was estimated by extrapolating the initial slope of its binding curve to a zero C_f value. The estimated partition coefficients, K_p*, of NBD-SV-269 were 2.2×10^4 and 5.0×10^4 in PS/PC and PC vesicles, respectively, and those of NBD-MuSV-269 were 3.0×10^4 and 5.8×10^4 in PS/PC and PC vesicles, respectively. These values are high and are typical for surface-active peptides (*45*, *34*, *46*). It should be noted that the high quantum yield of NBD fluorescence in the phospholipid membranes permits the use of low concentrations of NBD-labeled peptides and thus reduces peptide aggregation in solution. However, we cannot rule out that some aggregation of the peptides does occur in solution at these low concentrations as discussed earlier. It should also be emphasized that the purpose of the binding experiments was to determine the lipid:peptide molar ratios at which most of the peptides bound to the membranes. These ratios were then used in the resonance energy transfer

experiments to ensure correct calculation of the percentage of energy transfer.

The shape of a binding isotherm of a peptide provides information on the organization of the peptide within the membrane (*35*). The linear nature of the binding isotherms of SV-269 in PC vesicles and MuSV-269 in PC and PS/PC vesicles (Figure 4B) indicates a simple adhesion process (*35*), suggesting that the wild-type peptide in PC vesicles and the mutant peptide in either PS/PC or PC vesicles do not form large aggregates. However, the binding isotherm of SV-269 reflects cooperativity in the binding process in PS/PC vesicles (Figure 4B) (*35*).

SV-269, but Not MuSV-269, Self-Associates and Coassembles with the Heptad Repeats SV-150 in Membranes—Resonance Energy Transfer Experiments. The shape of a binding isotherm shows whether a particular peptide binds to the membrane in a cooperative manner and forms large aggregates. However, a binding isotherm cannot ascertain self-association of a particular polypeptide to form small sized bundles, or heteroassociation of several distinct monomers. To examine this possibility, RET experiments were performed with NBD-labeled peptides serving as energy donors, and Rho-labeled peptides serving as energy acceptors. Typical profiles of energy transfer experiments for SV-269 and MuSV-269 in the presence of PS/PC vesicles are shown in Figure 5A upper and lower panels, respectively. Addition of Rho-SV-269 or Rho-MuSV-269 (final concentration of 0.087−0.60 μM) to the corresponding donors, NBD-SV-269 and NBD-MuSV-269, respectively (final concentrations of 0.09 and 0.11 μM, respectively) in the presence of or PS/PC (Figure 5A) or PC (profiles not shown) phospholipid vesicles (288 μM), quenched the donor's emission and increased the acceptor's emission, consistent with energy transfer. The data reveal that the observed energy transfer, which is measured by the decrease of the donor fluorescence following the addition of the acceptor peptide, is much lower for MuSV-269 than that observed with SV-269. Furthermore, to check whether the leucine zipper motif SV-269 could coassemble with other domains of Sendai virus fusion protein, energy transfer experiments were performed between SV-269 or mutant MuSV-269, and the two heptad repeats SV-150 and SV-473. In these experiments, NBD-labeled wild-type or mutant SV-269 peptides were used as energy donors and Rho-labeled heptad repeats, as energy acceptors. A significant energy transfer was observed only between NBD-SV-269 and the Rho-labeled heptad repeat SV-150 in PS/PC and PC vesicles. However, no significant energy transfer was observed between the NBD-MuSV-269 and the two heptad repeats in either PS/PC or PC vesicles. The curves of the experimentally derived percentage of energy transfer versus the of bound-acceptor:lipid molar ratio are shown in Figure 5B. The molar concentration of the bound acceptor was estimated using the corresponding binding isotherm, as described previously (*43*). High lipid:peptide molar ratios (~3000:1) were used in these experiments to ensure (i) that practically all the peptides were in their membrane-bound state, (ii) that there was a low surface density of donors and acceptors which would reduce energy transfer between unassociated peptide monomers, and (iii) that the morphology of the vesicles was not altered (as confirmed by negative-staining electron microscopy; data not shown). Adding the acceptor-peptide only after the donor-peptide was already bound to

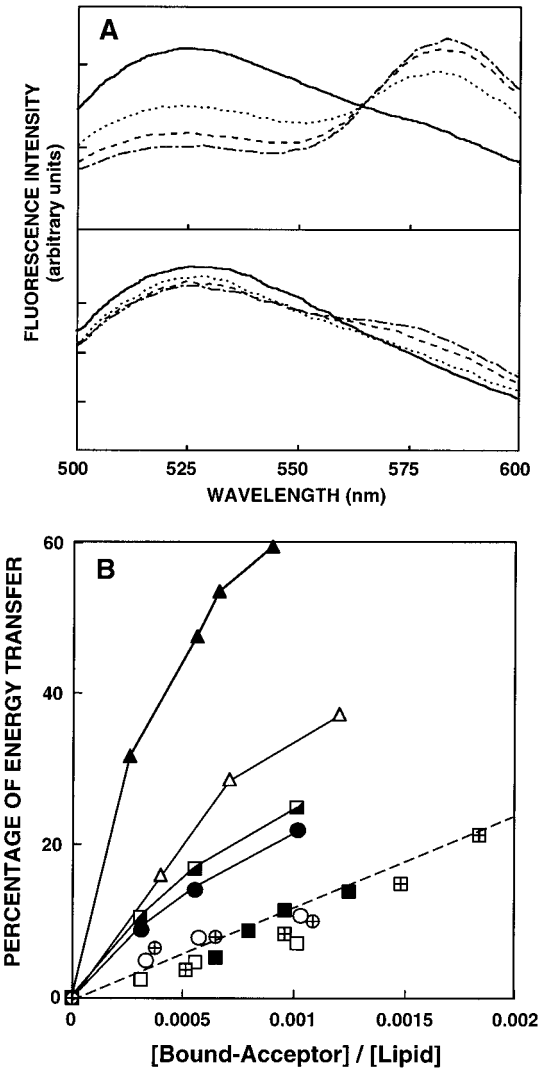

FIGURE 5: (A) Dependence of fluorescence energy transfer on the Rho-peptide (acceptor) concentration in the liposomes. The spectra were recorded for the donor-peptide alone and in the presence of various amounts of an acceptor-peptide. The excitation wavelength was set at 467 nm, and the emission was scanned from 500 to 600 nm. (Upper panel) The spectrum of NBD-SV-269 (0.09 μM) in the presence of PS/PC (1:1) SUV (288 μM) alone (—), and with various concentrations of Rho-SV-269; (•••) 0.0837 μM; (---) 0.251 μM; and (— •—) 0.335 μM. (Lower panel) The spectrum of NBD-MuSV-269 (0.11 μM) alone (—) in the presence of PS/PC (1:1) SUV (360 μM) and various concentrations of Rho-MuSV-269; (•••) 0.30 μM, (---) 0.45 μM; and (— • —) 0.60 μM. (B) Theoretically- and experimentally-derived percentages of energy transfer. The percentage of energy transfer was calculated (described under Materials and Methods), and was plotted versus the molar ratio between the bound-acceptor and the lipids. The amounts of lipid-bound acceptor (Rho-peptides), C_b, at various acceptor concentrations were calculated from the binding isotherms as described previously (*43*). Symbols: Filled triangles, NBD-SV-269/Rho-SV-269 in PS/PC SUV; open triangles, NBD-SV-269/Rho-SV-269 in PC SUV; half-filled squares, NBD-SV-269/Rho-SV-150 in PS/PC SUV; crossed circles, NBD-MuSV-269/Rho-SV-150 in PS/PC SUV; filled circles, NBD-SV-269/Rho-SV-150 in PC SUV; open circles, NBD-Mu-SV-269/Rho-SV-150 in PC SUV; filled squares, NBD-MuSV-269/Rho-MuSV-269 in PS/PC SUV; open squares, NBD-MuSV-269/Rho-MuSV-269 in PC SUV; crossed squares, NBD-SV-269/Rho-SV-473 in PS/PC SUV; dashed line, random distribution of the monomers (*47*), assuming a R_0 of 51 Å. Energy transfer data of NBD-MuSV-269/Rho-SV-473 in PS/PC SUV and of NBD-SV-269/Rho-SV-473 and NBD-MuSV-269/Rho-SV-473 in PC SUV come from below the random distribution level and were not shown to prevent clustering.

the membrane prevented any association of the peptides in solution. In order to confirm that the observed energy transfer was due to association of peptides, the energy transfer efficiencies observed for the peptides were compared with those expected for randomly-distributed membrane-bound donors and acceptors. A curve corresponding to the random distribution of monomers, described by Fung and Stryer (*47*), was calculated with an assumed R_0 value of 51 Å for the NBD/Rho donor/acceptor pair, as calculated previously (*48*) (dashed line in Figure 5B). The percentages of energy transfer observed with NBD-SV-269/Rho-SV-269 and NBD-SV-269/Rho-SV-150 in PC or PS/PC vesicles are higher than the energy transfer expected for the random distribution of monomers. However, the observed energy transfers between NBD-SV-269/Rho-SV-473, NBD-MuSV-269/Rho-MuSV-269, NBD-MuSV-269/Rho-SV-150, and NBD-MuSV-269/Rho-SV-473 in both PC and PS/PC vesicles are similar to that observed for random distribution (Figure 5B). The emission spectrum of the donor did not change when an equal amount of unlabeled acceptor was added instead of the Rho-labeled acceptor (data not shown). In summary, these energy transfer experiments reveal that the wild-type leucine zipper motif can self-assemble and coassemble with heptad repeat SV-150 in both zwitterionic and negatively-charged phospholipid vesicles. However, the mutant peptide can neither self-assemble nor coassemble with other regions in either PC or PS/PC phospholipid vesicles.

Susceptibility of Membrane-Bound SV-269 and MuSV-269 to Proteolytic Cleavage. To determine whether the peptides are exposed to the aqueous phase in their membrane-bound state, NBD-labeled peptides were treated with the proteolytic enzyme proteinase K before and after binding to phospholipid membranes. Figure 6A depicts one such experimental profile for the wild-type SV-269. NBD-labeled peptide was first added to PBS (time point 1), followed by the addition of PS/PC vesicles (time point 2), which caused a large increase in fluorescence. Once the curve reached a plateau, indicating the completion of binding of NBD-labeled peptides to the membrane, proteinase K was added (time point 3) to the peptide−lipid complex. Figure 6A shows that after proteinase K treatment, the fluorescence of the NBD-labeled peptide decreased. This indicates that the labeled peptide is exposed to the aqueous phase and is susceptible to degradation in its membrane-bound state. Similar results were obtained with NBD-MuSV-269 (Figure 6C). These observations suggest that major portions of both wild-type and mutant leucine zipper regions are located on the surface of the PS/PC vesicles and therefore are accessible to proteinase K. Control experiments were done by adding proteinase K to NBD-labeled peptides prior to the addition of vesicles (Figure 6B,D). When PS/PC vesicles were added (time point 2 of Figure 6B,D) to degraded peptides, a small increase of fluorescence was observed due to binding of partially uncleaved peptides to vesicles. Similar results were obtained when zwitterionic PC vesicles were used instead of negatively charged PS/PC vesicles (data not shown).

Both Wild-Type and Mutant SV-269 Can Permeate Membranes. Whether wild-type or mutant leucine zipper regions perturb the packing of the phospholipid membranes was determined by the efficacy of the peptides and their fluorescent derivatives to dissipate the diffusion potential from SUVs composed of PC or PS/PC. Increasing concentrations of the peptides were added to PC or to PS/PC SUVs

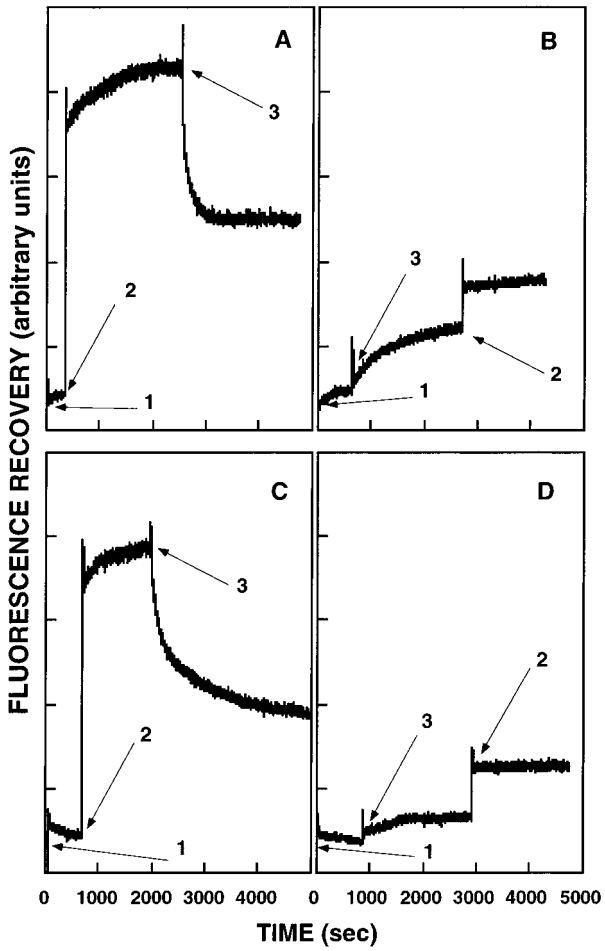

FIGURE 6: Determination of the location of wild-type, SV-269 (panel A), and mutant, MuSV-269 (panel C), peptides by studying the proteolytic digestion of NBD-labeled analogues in the presence of PS/PC vesicles. In control experiments, proteinase K was added to NBD-SV-269 (panel B) and NBD-MuSV-269 (panel D) in buffer prior to the addition of lipid vesicles. The fluorescence intensity of the labeled peptide was monitored at 530 nm with the excitation set at 467 nm. The digestion was performed in 150 mM NaCl, 10 mM sodium phosphate, pH 7.3. 1, 2, and 3 indicate the addition of NBD-SV-269 (or NBD-MuSV-269), SUV, and proteinase K, respectively. The concentration of either NBD-SV-269 or NBD-MuSV-269 was 0.1 μM, and that of PS/PC SUV was fixed at 288.0 μM.

pretreated with a fluorescent, potential sensitive dye, diS-C_2-5, and valinomycin. Fluorescence recovery due to membrane permeability induced by the peptides was monitored as a function of time until a plateau was reached (usually within 30−50 min after the addition of peptide). Both the wild-type and mutant leucine zipper motifs and their fluorescent derivatives induced the dissipation of the diffusion potential in PC and PS/PC vesicles (figure not shown). Both wild-type and mutant peptides showed 50% activity at lipid:peptide ratios of ∼20:1 and 10:1, in PS/PC and PC, respectively.

Secondary Structures of the Peptides. The extent of α-helical secondary structure of SV-269 and MuSV-269 was estimated from their CD spectra, as measured in buffer, 40% TFE, 1% SDS, and in the presence of PS/PC vesicles (Figure 7). The mean residual ellipticity of the wild-type SV-269 in 40% TFE at 222 nm, $[\Theta]_{222}$, was −8900, which corresponds to 23% helicity. This signal increased slightly in 1% SDS, corresponding to 28% helicity. The mean residual ellipticity, $[\Theta]_{222}$,of MuSV-269 in both 40% TFE and 1%

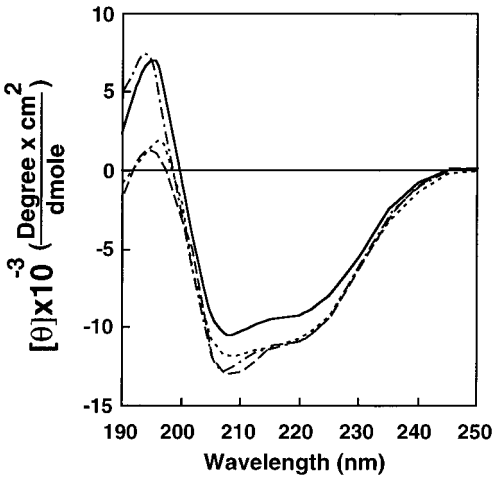

FIGURE 7: CD spectra of SV-269 and MuSV-269 in different environments. Spectra were recorded at peptide concentrations of 11.4 μM for both SV-269 and MuSV-269. Symbols: (—) SV-269 in 40% TFE; (•••) SV-269 in 1% SDS; (— • —) MuSV-269 in 40% TFE; and (— —) MuSV-269 in 1% SDS.

SDS was ~10 500, which corresponds to 29% α-helix structure. SV-269 exhibited very low mean residual ellipticities at 222 nm both in PBS and in the presence of PS/PC vesicles (up to a lipid:peptide molar ratio of 150; spectra not shown). MuSV-269 also did not exhibit a significant CD signal either in PBS or in the presence of PS/PC vesicles. It should be noted that under these conditions, only a fraction of the peptide is bound to the vesicles (see binding curve in Figure 4). An increase in the concentration of the vesicles caused significant light scattering which did not allow CD measurements.

SV-269, but Not MuSV-269, Binds to Sendai Virus. In the previous experiments, we showed that SV-269 self-assembles and coassembles with two other heptad repeats in aqueous solution and in membrane as well. However, the mutant peptide MuSV-269 neither self-assembles nor coassembles with other domains of the Sendai virus fusion protein in solution or in membranes. We therefore investigated whether SV-269 can recognize its counterpart or the two heptad repeats of the envelope protein of the Sendai virus in its activated or nonactivated form. For this purpose, NBD-labeled peptides were used. The assay was developed with the assumption that binding of NBD-labeled peptide to virions will decrease the amount of free NBD-labeled peptide in solution that can bind to phospholipid vesicles. Under these conditions, the increase in the fluorescence of the NBD-labeled peptide is expected to be lower than that observed in the absence of virions, and when all the NBD-labeled peptide is bound to the vesicles. The results of these experiments are summarized in Figure 8A. The first column shows the fluorescence of NBD-labeled wild-type peptide in its membrane-bound state, in the absence of added virions. When NBD-SV-269 was first treated with virions and only then vesicles were added, the observed fluorescence of NBD-SV-269 (marked by NBD-SV-269 + virions) was only ~50% of that of the first column. This result indicates that at least some of the wild-type peptide was bound to virions and therefore not able to interact with the lipid vesicles. Interestingly, when the peptide was treated with inactivated virions (virions incubated at 65 °C for 20 min), the level of NBD fluorescence in the presence of lipid vesicles was higher than that obtained with active virions. These results reveal

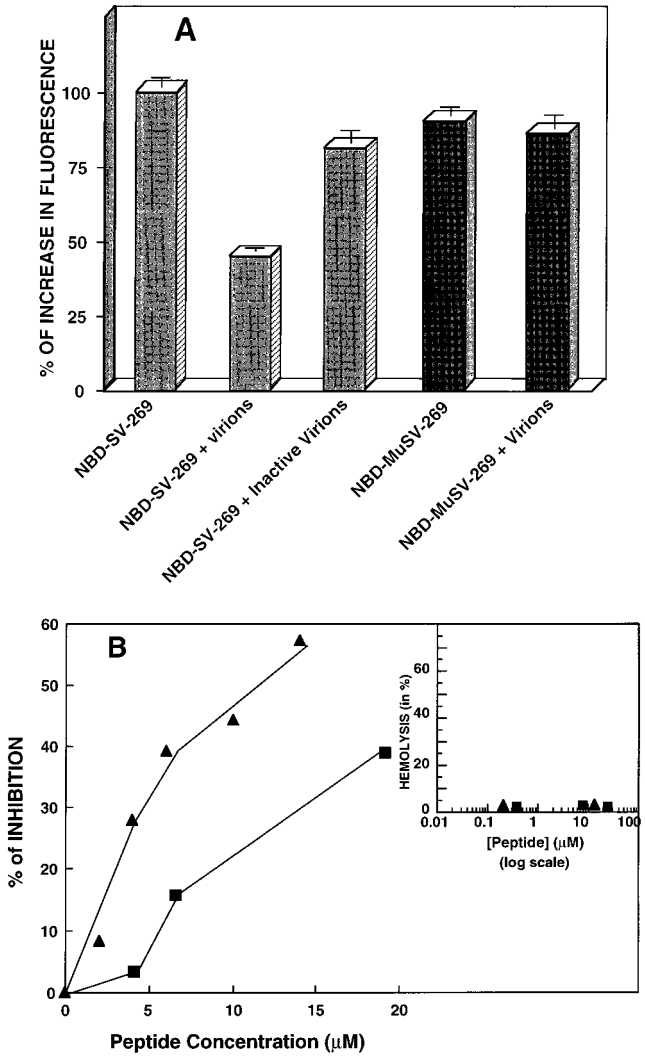

FIGURE 8: (A) Detection of the binding of Sendai virus to the wild-type or mutant leucine zipper motif by comparing the percentage of increase in the fluorescence of NBD-labeled peptides in the presence of PS/PC vesicles, before and after incubation of virions. Virions were incubated with NBD-labeled peptides for 30 min followed by the addition of vesicles, and then NBD fluorescence was recorded until a plateau was reached. Concentrations of NBD-labeled peptides, PS/PC vesicles, and virions were fixed at 0.1 μM, 288 μM, and 48 HAU, respectively. The virions were inactivated by incubating them at 65 °C for 20 min. (B) Dose response of the inhibition potential of SV-269 and MuSV-269. Various amounts of peptides were added to duplicate samples of virions in 100 μL of PBS and incubated for 20 min at room temperature. RBCs (125 μL 4%) were then added to the mixtures of peptides and virions and incubated for 10 min at room temperature, followed by incubation at 37 °C for 40 min and finally centrifuged for 8 min at 5700*g*. The inhibition of hemolysis was calculated from the recorded absorbance of the supernatants at 540 nm. Symbols: triangles, SV-269; squares, MuSV-269. Inset: percent of the hemolytic activity of the peptides alone expressed as a function of their concentration; triangles, SV-269; squares, MuSV-269.

that SV-269 only binds to activated virus. Similar experiments were done with NBD-MuSV-269. The observed fluorescence of the same amount of NBD-MuSV-269, treated with virions, in the presence of lipid vesicles is only slightly lower than that obtained in the absence of virions (Figure 8A, fourth and fifth columns). This reflects that the mutant peptide does not significantly bind to the virions.

SV-269 Is More Potent Than MuSV-269 in Inhibiting Sendai Virus Mediated Hemolysis of Human RBC. The hemolytic activity of Sendai virus is associated with fusion

Table 3: Summary of the Different Properties of SV-269 and MuSV-269

	SV-269			MuSV-269		
peptides' property	solution	PC	PS/PC	solution	PC	PS/PC
membrane binding	/	+	+	/	+	+
membrane localization	/	surface	surface	/	surface	surface
membrane permeation	/	+	+	/	+	+
binding to active Sendai virus	+	/	/	−	/	/
binding to inactive Sendai virus	−	/	/	−	/	/
self-assembly	+++	+	+	+/−	−	−
assembly with SV-150	+	+	+	−	−	−
assembly with SV-473	+	−	−	−	−	−
inhibition activity	+++	/	/	+	/	/

of the virus with target red blood cells (RBC) (*49*). To further study the inhibition potential of SV-269 and MuSV-269, Sendai virus mediated hemolysis was assayed in the presence of these peptides. The assay was performed as follows: virions were initially incubated with RBCs at room temperature to allow their attachment to the cells. Subsequent incubation at 37 °C resulted in RBC lysis. The extent of lysis was measured by the absorbance at 540 nm (characteristic of hemoglobin). To investigate the inhibition potential of SV-269 and MuSV-269, the peptides were incubated with virions for 20 min followed by the addition of RBCs. Figure 8B depicts the dose response inhibitory effect of the peptides on the hemolytic activity of Sendai virus. The data reveal that SV-269 is significantly more potent than MuSV-269 in the inhibition assay. The difference in their activities is more pronounced in the lower concentration range in which MuSV-269 has only ~13% of the activity of the wild-type peptide. The inset shows that both wild-type and mutant peptides had no hemolytic activity up to the maximum concentration tested (100 μM), thus eliminating the possibility that they contribute to the hemolytic activity during the fusion process.

DISCUSSION

We have identified a highly conserved leucine zipper motif in the ectodomain of the Sendai virus, synthesized it, and investigated its possible involvement in the assembly of the Sendai virus fusion protein. A mutant peptide, MuSV-269, with only two amino acids (one heptadic leucine and a glutamic acid), interchanged in their positions was also investigated. The similarities and distinctions between the physicochemical properties of the wild-type SV-269 and the mutant MuSV-269 shown in Table 3 are discussed below in light of a possible role of SV-269 in the assembly of the fusion protein in solution and membranes. Fluorescence studies using Rho-labeled peptide demonstrate that the wild-type leucine zipper motif, SV-269, exists in an aggregated state while the mutant peptide, MuSV-269, is not significantly assembled in aqueous solution. Since SV-269 and MuSV-269 peptides are of the same size and possess the same hydrophobicity, we may conclude that the specific sequence of SV-269 is responsible for the self-association of the peptide in solution. Furthermore, the exchange of Rho-SV-269 with unlabeled peptides when mixed together (Figure 2A) reveals that SV-269 can self-assemble in a reversible manner. Interestingly, SV-269, but not MuSV-269, can also coassemble in solution with two biologically-active heptad repeat regions, SV-150 and SV-473, but cannot coassemble with a shorter version of SV-150, namely, SV-163 (Figure 2B), which was shown to be biologically-inactive (*21*). This was further supported by circular dichroism studies (Figure 3). When SV-269, but not MuSV-269, was mixed with either SV-150 or SV-473, the CD spectra exhibited a significant increase in ellipticity values compared to the algebric sum of the individual spectrum of each pair. The specificity of these interactions may indicate that SV-269 can work together with the heptad repeats to stabilize the Sendai virus fusion protein in the native state. These results are consistent with the notion that enveloped-virus fusion proteins are oligomeric which is convenient for the liberation of a fusion peptide and cellular transport (*39*). The leucine zipper motifs which have been proposed to be involved in the fusogenic assembly of influenza hemagglutinin (*23*) or the heptad repeat SV-473 of the Sendai virus fusion protein (*21*) are also aggregated in solution.

Using fluorescence energy transfer experiments, we found that only SV-269 but not MuSV-269 can self-assemble or coassemble with the heptad repeat SV-150 in both zwitterionic and negatively-charged phospholipid membrane (Figure 5B). This led us to speculate that SV-269 may also participate in the assembly of the Sendai virus fusion protein in the membrane. Since MuSV-269, which has the same amino acid content as the wild type, cannot self-associate or coassemble with other domains either in aqueous solution or in the membrane, it can be concluded that the heptadic leucine at position 285 plays a crucial role in the assembly of the leucine zipper motif. That this leucine zipper motif can self- and coassemble with other domains of the Sendai virus fusion protein is supported by the finding that NBD-labeled wild-type SV-269 binds to Sendai virions (Figure 8A). As expected, viral binding ability is almost negligible in the mutant peptide. Moreover, NBD-SV-269 did not bind significantly to inactivated virions, demonstrating the specific nature of this binding. Most probably, the envelope protein of the inactivated virus loses its native conformation and thus is not recognized by the wild-type leucine zipper motif. It is reasonable to assume that the binding of SV-269 to Sendai virus is due to its recognition of its counterpart or one of the heptad repeats in the envelope protein of Sendai virus. This finding further supports the possibility that the SV-269 leucine zipper motif can participate in subunit interactions and thus stabilize the oligomeric structure of the fusion protein in its native state. We further found that SV-269 can inhibit the Sendai virus-mediated hemolysis in a dose-dependent manner, whereas the mutant MuSV-269 was significantly less active (Figure 8B).

A leucine zipper motif is reported to be helical coiled-coil. However, the CD spectra of SV-269 showed low helical content in PBS (Figure 7). Similar data were reported for a predicted α-helical domain, DP-178, of the HIV transmembrane protein gp41 (*20*), which according to the Lupas Algorithm DP-178 should be helical in aqueous solution. One of the reasons for the low helical structure of SV-269 could be the presence of two prolines in this sequence. The prolines could induce bending in the helical secondary structure of the SV-269 which would lower the helical content of the peptide as compared to an elongated helix. This is consistent with the observation that a bend along an α-helix causes a significant reduction in its mean residual ellipticity (*50*). Interestingly, one of the prolines (position 290) is conserved not only in the Sendai virus

family but also in the corresponding regions of other paramyxoviruses like rinderpest, measles, parainfluenza, and simian virus 5. The second proline, located at position 296, is also conserved in parainfluenza and SV5 viruses (Table 1).

The hydropathy plot of the Sendai virus fusion protein suggests that besides the fusion peptide and the transmembrane anchor domain, there are other sufficiently hydrophobic regions that could be involved in membrane binding during fusion (*51*). SV-269, a leucine zipper motif, is one of the possible regions which we found to bind both the negatively charged and zwitterionic phospholipid membranes. Recently, Durrer et al. (*52*), using a radiolabeled photoaffinity reagent, showed that during low-pH-induced membrane insertion of influenza virus hemagglutinin, only the N-terminal fusion peptide of the fusion protein inserts into the membrane. Membrane fusion mediated by Sendai virus envelope protein occurs at neutral pH, and, therefore, the mechanism of low-pH-induced influenza hemagglutinin-mediated membrane fusion may not be applicable. Furthermore, the radiolabeled photoaffinity reagent is inserted into the hydrophobic part of the membrane, and therefore may be more efficient in detecting membrane-inserting domains but not domains that participate in the fusion event by positioning themselves on the surface of the membrane. Blue shift experiments using NBD-labeled peptides demonstrate that the N-terminal of SV-269 is located close to the surface of the membrane. Addition of proteinase K to membrane-bound NBD-labeled peptide resulted in a decrease of the NBD fluorescence, further indicating that the peptide is located on the membrane surface (Figure 6). It is possible that this leucine zipper-like motif, which is capable of binding to the surface of membrane, lies on the surface of the target membrane and assists in the apposition of the viral and target membranes. A similar role was suggested for leucine zipper motifs in the influenza hemagglutinin (*24*) and HIV gp41 (*53*) due to their ability to bind membrane.

Prior to the merging of the target and viral membranes, it is believed that the fusion protein destabilizes the target membrane. In addition, fusion pores were detected in membrane fusion mediated by influenza hemagglutinin and baculovirus GP64 (*54*, *55*). However, the molecular mechanism associated with the disintegration of the target membrane is not clearly understood. Our observation that the leucine zipper SV-269 can cause leakage of either negatively charged or zwitterionic phospholipid vesicles suggests that this region of the Sendai virus fusion protein may be also involved in destabilizing the target membrane.

In summary, we have identified a leucine zipper motif in the ectodomain of the Sendai virus which is extremely conserved in the family of Sendai viruses. Furthermore, most of the heptadic leucines are also conserved in other paramyxoviruses. Our results suggest that this domain might be associated with the assembly of fusion protein in its native state as well as within the membrane. Furthermore, we propose that this region may be associated with the destabilization of the target membrane and assists in the apposition of membranes during fusion, and that the homologous leucine zipper motifs in other viruses may play a similar role.

REFERENCES

1. Stegmann, T., Doms, R. W., and Helenius, A. (1989) *Annu. Rev. Biophys. Biophys. Chem. 18*, 187−211.
2. White, J. M. (1990) *Annu. Rev. Physiol. 52*, 75−97.
3. Hoekstra, D., and Kok, J. W. (1989) *Biosci. Rep. 9*, 273−305.
4. Lamb, R. A. (1993) *Virology 197*, 1−11.
5. Scheid, A., and Choppin, P. W. (1974) *Virology 57*, 475−490.
6. Haywood, A. M. (1974) *J. Mol. Biol. 83*, 427−436.
7. Klenk, H. D., Rott, R., Orlich, M., and Blodorn, J. (1975) *Virology 68*, 426−439.
8. Homma, M., and Ohuchi, M. (1973) *J. Virol. 12*, 1457−1465.
9. Scheid, A., and Choppin, P. W. (1977) *Virology 80*, 54−60.
10. Landschultz, W. H., Johnson, P. E., and Mcknight, S. L. (1988) *Science 240*, 1759−1764.
11. O'Neil, K. T., Hoess, R. H., and DeGrado, W. F. (1990) *Science 249*, 774−778.
12. Johnson, P. F., and Mcknight, S. L. (1989) *Annu. Rev. Biochem. 58*, 799−839.
13. O'Shea, E. K., Rutkowski, R., and Kim, P. K. (1989) *Science 243*, 538−542.
14. Bernstein, H. B., Tucker, S. P., Kar, S. R., McPherson, D. T., Dubay, J. W., Lebowitz, J., Compans, R. W., and Hunter, E. (1995) *J. Virol. 69*, 2745−2750.
15. Shugars, D. C., Wild, C. T., Greenwell, T. K., and Matthews, T. J. (1996) *J. Virol. 70*, 2982−2991.
16. Chen, S. S., Lee, C. N., Lee, W. R., McIntosh, K., and Lee, T. H. (1993) *J. Virol. 67*, 3615−3619.
17. Buckland, R., Malvoisin, E., Beauverger, P., and Wild, F. (1992) *J. Gen. Virol. 73*, 1703−1707.
18. Reitter, J. N., Sergel, T., and Morrison, T. G. (1995) *J. Virol. 69*, 5995−6004.
19. Wild, C., Oas, T., McDanal, C., Bolognesi, D., and Matthews, T. (1992) *Proc. Natl. Acad. Sci. U.S.A. 89*, 10537−10541.
20. Wild, C. T., Shugars, D. C., Greenwell, T. K., McDanal, C. B., and Matthews, T. J. (1994) *Proc. Natl. Acad. Sci. U.S.A. 91*, 9770−9774.
21. Rapaport, D., Ovadia, M., and Shai, Y. (1995) *EMBO J. 14*, 5524−5531.
22. Lambert, D. M., Barney, S., Lambert, A. L., Guthrie, K., Medinas, R., Davis, D. E., Erickson, T. B., Merutka, G., and Petteway, S. R., Jr. (1996) *Proc. Natl. Acad. Sci. U.S.A. 93*, 2186−2191.
23. Carr, C. M., and Kim, P. S. (1993) *Cell 73*, 823−832.
24. Yu, Y. G., King, D. S., and Shin, Y.-K. (1994) *Science 266*, 274−276.
25. Merrifield, R. B., Vizioli, L. D., and Boman, H. G. (1982) *Biochemistry 21*, 5020−5031.
26. Shai, Y., Bach, D., and Yanovsky, A. (1990) *J. Biol. Chem. 265*, 20202−20209.
27. Rapaport, D., and Shai, Y. (1992) *J. Biol. Chem. 267*, 6502−6509.
28. Peretz, H., Toister, Z., Laster, Y., and Loyter, A. (1974) *J. Cell Biol. 63*, 1−11.
29. Shai, Y., Hadari, Y. R., and Finkels, A. (1991) *J. Biol. Chem. 266*, 22346−22354.
30. Bartlett, G. R. (1959) *J. Biol. Chem. 234*, 466−468.
31. Papahadjopoulos, D., and Miller, N. (1967) *Biochim. Biophys. Acta 135*, 624−638.
32. Greenfield, N., and Fasman, G. D. (1969) *Biochemistry 8*, 4108−4116.
33. Wu, C. S. C., Ikeda, K., and Yang, J. T. (1981) *Biochemistry 20*, 566−570.
34. Rapaport, D., and Shai, Y. (1991) *J. Biol. Chem. 266*, 23769−23775.
35. Schwarz, G., Gerke, H., Rizzo, V., and Stankowski, S. (1987) *Biophys. J. 52*, 685−692.
36. Beschiaschvili, G., and Seelig, J. (1990) *Biochemistry 29*, 52−58.
37. Sims, P. J., Waggoner, A. S., Wang, C. H., and Hoffmann, J. R. (1974) *Biochemistry 13*, 3315−3330.
38. Loew, L. M., Rosenberg, I., Bridge, M., and Gitler, C. (1983) *Biochemistry 22*, 837−844.
39. Doms, R. W., Lamb, R. A., Rose, J. K., and Helenius, A. (1993) *Virology 193*, 545−562.

40. Lawless, M. K., Barney, S., Guthrie, K. I., Bucy, T. B., Petteway, S. R., and Merutka, G. (1996) *Biochemistry 35*, 13697−13708.
41. Kenner, R. A., and Aboderin, A. A. (1971) *Biochemistry 10*, 4433−4440.
42. Frey, S., and Tamm, L. K. (1990) *Biochem. J. 272*, 713−719.
43. Pouny, Y., Rapaport, D., Mor, A., Nicolas, P., and Shai, Y. (1992) *Biochemistry 31*, 12416−12423.
44. Rajarathnam, K., Hochman, J., Schindler, M., and Ferguson, M. S. (1989) *Biochemistry 28*, 3168−3176.
45. Rizzo, V., Stankowski, S., and Schwarz, G. (1987) *Biochemistry 26*, 2751−2759.
46. Gazit, E., and Shai, Y. (1993a) *Biochemistry 32*, 3429−3436.
47. Fung, B. K., and Stryer, L. (1978) *Biochemistry 17*, 5241−5248.
48. Gazit, E., and Shai, Y. (1993b) *Biochemistry 32*, 12363−12371.
49. Loyter, A., and Volsky, D. J. (1982) *Cell Surf. Rev. 8*, 215−266.
50. Hirst, J. D., and Brooks, C. L., III (1994) *J. Mol. Biol. 243*, 173−178.
51. Blumberg, B. M., Giorgi, C., Rose, K., and Kolakofsky, D. (1985) *J. Gen. Virol. 66*, 317−331.
52. Durrer, P., Galli, C., Hoenke, S., Corti, C., Gluck, R., Vorherr, T., and Brunner, J. (1996) *J. Biol. Chem. 271*, 13417−13421.
53. Rabenstein, M., and Shin, Y.-K. (1995) *Biochemistry 34*, 13390−13397.
54. Spruce, A. E., Iwata, A., White, J. M., and Almers, W. (1989) *Nature 342*, 555−558.
55. Plonsky, I., and Zimmerberg, J. (1996) *J. Cell Biol. 135*, 1831−1839.

BI971152I